

# Mutational Analysis of the P1 Phosphorylation Domain in *Escherichia coli* CheA, the Signaling Kinase for Chemotaxis

So-ichiro Nishiyama,\* Andrés Garzón,\* John S. Parkinson

Department of Biology, University of Utah, Salt Lake City, Utah, USA

**The histidine autokinase CheA functions as the central processing unit in the *Escherichia coli* chemotaxis signaling machinery. CheA receives autophosphorylation control inputs from chemoreceptors and in turn regulates the flux of signaling phosphates to the CheY and CheB response regulator proteins. Phospho-CheY changes the direction of flagellar rotation; phospho-CheB covalently modifies receptor molecules during sensory adaptation. The CheA phosphorylation site, His-48, lies in the N-terminal P1 domain, which must engage the CheA ATP-binding domain, P4, to initiate an autophosphorylation reaction cycle. The docking determinants for the P1-P4 interaction have not been experimentally identified. We devised mutant screens to isolate P1 domains with impaired autophosphorylation or phosphotransfer activities. One set of P1 mutants identified amino acid replacements at surface-exposed residues distal to His-48. These lesions reduced the rate of P1 transphosphorylation by P4. However, once phosphorylated, the mutant P1 domains transferred phosphate to CheY at the wild-type rate. Thus, these P1 mutants appear to define interaction determinants for P1-P4 docking during the CheA autophosphorylation reaction.**

Chemotaxis, movement toward beneficial chemicals or away from harmful ones, is an important adaptive behavior of motile bacteria. Chemotactic behaviors have been documented in a number of bacteria but have been most extensively studied in *Escherichia coli* (1). *E. coli* has one set of chemotaxis genes whose products comprise a simple signaling pathway in which the histidine autokinase CheA serves as the central processing unit (2). CheA operates as a homodimer; each subunit contains five functional domains, designated P1 to P5 (Fig. 1A). P3 comprises the main dimerization determinants; P1 contains the site of autophosphorylation, His-48; P4 is the ATP-binding domain. During CheA autophosphorylation, a *trans* reaction, the P1 domain of one subunit interacts with the P4 domain of the other subunit (Fig. 1B) (3).

Transmembrane chemoreceptor proteins monitor the external levels of chemoeffector compounds, such as the amino acid attractants serine and aspartate. The cytoplasmic tips of the receptor molecules form ternary signaling complexes with CheA and with CheW, which couples CheA activity to receptor control (Fig. 1C). The P5 domain of CheA binds to both CheW and receptors and is critical for assembly and function of ternary signaling complexes (4, 5). Ligand-free receptors activate CheA autophosphorylation several hundred-fold over its basal, uncoupled rate. Attractant-occupied receptors deactivate CheA to below its basal rate. Phospho-CheA donates its phosphoryl groups to two response regulators, CheY and CheB, which reversibly bind to the CheA-P2 domain, increasing their local concentration at the receptor signaling complex (Fig. 1B). Phospho-CheY binds to the switch components of the flagellar motor to promote clockwise (CW) rotation, which causes the cell to tumble and randomly change its swimming direction. Counterclockwise (CCW) rotation of the flagellar motors, the default behavior, produces forward swimming episodes. CheB, a receptor methyl-erastase, and CheR, a methyltransferase, comprise a negative feedback loop that covalently modifies the receptor signaling domain to terminate stimulus responses. Sensory adaptation allows cells to monitor changes in chemical concentrations and thereby track spatial che-

moeffector gradients as they swim about. Phosphorylation enhances CheB activity to accelerate the adaptation process.

The mechanism of CheA regulation in ternary signaling complexes might involve allosteric control of the CheA autophosphorylation reaction. For example, receptors and CheW might manipulate, either directly or indirectly, interactions between the P1 and P4 domains of CheA. The CheA structural determinants that promote the P1-P4 interaction have not been experimentally identified, although cysteine-directed modifications (6) and docking simulations (7) have defined possible interaction surfaces on the two domains.

The covalent connection between P1 and the rest of the CheA molecule is not essential for the autophosphorylation reaction (8, 9), implying that the P1-P4 docking determinants alone have sufficient strength and specificity to promote functional interactions between the two domains. Moreover, isolated P1 fragments that have been phosphorylated in *trans* can donate their phosphoryl groups to CheB and CheY, albeit with somewhat lower rates than for native CheA (10). Thus, when expressed at sufficiently high stoichiometries, isolated P1 domains can support chemotactic signaling via interaction with an unconnected P4 domain. In the present work, we exploited these P1 signaling properties to identify P1 residues that are important for functional interaction with the P4 domain.

Received 30 September 2013 Accepted 23 October 2013

Published ahead of print 25 October 2013

Address correspondence to John S. Parkinson, parkinson@biology.utah.edu.

\* Present address: So-ichiro Nishiyama, Department of Frontier Bioscience, Hosei University, Tokyo, Japan; Andrés Garzón, Department of Molecular Biology & Biochemical Engineering, Pablo Olavide University, Seville, Spain.

Copyright © 2014, American Society for Microbiology. All Rights Reserved.

doi:10.1128/JB.01167-13

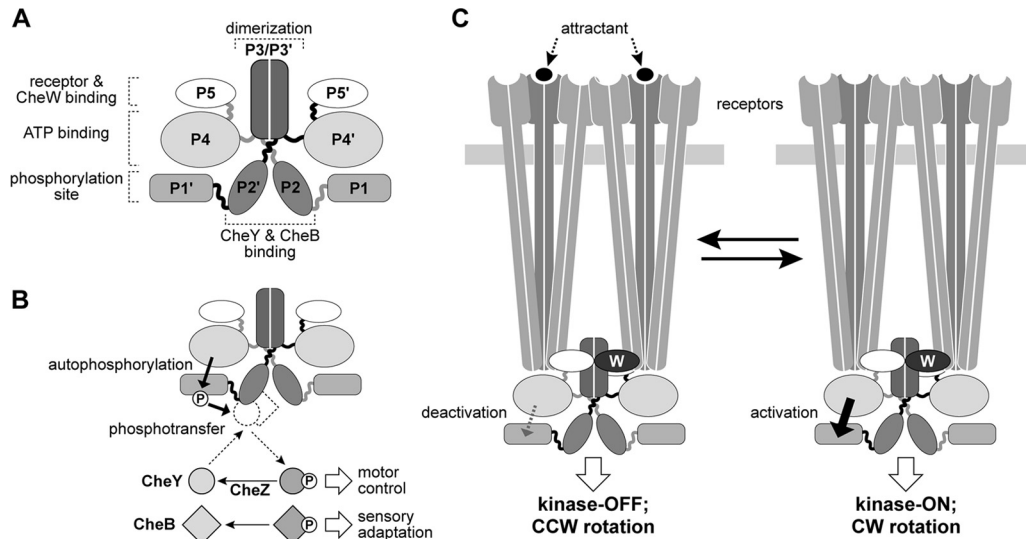


**FIG 1** Domain structure and signaling functions of CheA. (A) Functional architecture of the CheA homodimer. One CheA subunit is indicated with gray interdomain linkers, the other with black linkers. The central P3/P3' domains comprise the principal dimerization determinants. (B) CheA signaling reactions. Autophosphorylation of the homodimer occurs through a *trans* reaction between the P1 domain in one subunit and the P4 domain in the other. CheY and CheB catalyze the subsequent phosphotransfer reactions, using phospho-P1 as the phosphodonor. Transient docking of CheY and CheB to the CheA-P2 domains raises their local concentrations, accelerating phosphotransfer rates. (C) Chemoreceptor control of CheA activity. Chemoreceptor homodimers form trimers of dimers through interaction of their cytoplasmic tips. Two trimers of dimers bind two CheW monomers and one CheA dimer to form a signaling team, the minimal functional unit. Signaling teams in the CW output state activate CheA; teams in the CCW output state deactivate CheA. Stimuli and adaptational modifications shift teams between signaling states to control the cell's locomotor behavior.

## MATERIALS AND METHODS

**Bacterial strains and plasmids.** *E. coli* K-12 strains used in this work, and their relevant properties, were RP526 (*mutD5*) (11), RP437, our wild-type chemotaxis parental strain (12), and RP437 derivatives RP3098 [ $\Delta$ (*flhD-flhB*)4] (13), RP9535 (*cheA* $\Delta$ 1643) (14), RP9543 (*cheA* $\Delta$ 1643  $\Delta$ *cheZ*  $\Delta$ *tar-tap*  $\Delta$ *tsr*  $\Delta$ *trg*) (15), and UU1118 [*cheA* $\Delta$ (7-247)] (9).

Plasmids used to produce CheA and various CheA fragments were derivatives of pTM30, an isopropyl- $\beta$ -D-thiogalactopyranoside (IPTG)-inducible expression vector (8), or pKG116, a salicylate-inducible expression vector (16). pKJ9 carries the entire *cheA* coding region preceded by four in-frame codons of pTM30 (17). pAG3, encoding CheA1-149 (P1 domain), is a derivative of pKJ9 (9). pAG17, from pTM30-derived expression vector pCJ30 (18), also encodes CheA1-149 (this study). Plasmid pPA113 (pKG116 derived) expresses full-length *cheA* (4). Plasmid pSN9, encoding CheA260-654 (domains P3-P4-P5), is a derivative of pPA113 (this study). Plasmid pRL22 (19) is a tryptophan-inducible CheY expression vector.

**Media and culture conditions.** Tryptone broth contained 10 g/liter tryptone and 5 g/liter NaCl. HCG is H1 minimal salts medium (20) supplemented with 10 g/liter Casamino Acids and 4 g/liter glycerol. Liquid cultures were generally grown at 35°C.

**CheA-P1 mutant hunts.** DNA of plasmid pAG17 was mutagenized with hydroxylamine as previously described (21). The P1 coding regions were excised from the treated DNA by digestion with PstI and KpnI endonucleases and ligated to the complementary segment of unmutagenized pAG17 DNA. Independent plasmid pools were transferred to strain UU1118 by  $\text{CaCl}_2$  transformation and screened for chemotaxis-defective colonies on miniswarm plates (20). Samples of the transformation mixture were added to an empty petri dish and then mixed with 25 ml of tryptone broth containing 0.4% agar, 100  $\mu\text{g/ml}$  ampicillin, and 1 mM IPTG to induce P1 expression. After standing for several hours at room temperature to solidify, miniswarm plates were incubated at 35°C and screened the next day for small, nonchemotactic colonies among a diffuse background of chemotactic cells. The inoculum size was adjusted to yield about 5,000 to 10,000 transformant colonies per plate. Candidate mutants

were single-colony purified and retested for chemotaxis defects on tryptone soft agar at 32.5°C for 8 h and for expression of P1 polypeptides after IPTG induction in liquid culture (4). About half of the mutant candidates failed to express P1 protein and were discarded; the remainder of the mutant plasmids were subjected to DNA sequence analysis to identify mutational changes in their P1 coding regions.

In a second mutant hunt, plasmid pPA113 was mutagenized by propagation in RP526, a proofreading-deficient DNA polymerase mutant (11). The P1 coding region was excised from the treated DNA by digestion with NdeI and HpaI restriction endonucleases and ligated to the complementary segment of unmutagenized pPA113 DNA. Mutant plasmid pools were transformed into strain RP9543 and screened for enhanced pseudotaxis in miniswarm plates (see above) containing 10  $\mu\text{M}$  sodium salicylate.

**Transfer of the H26R allele from pPA113 to pAG17.** The P1 coding region of mutant plasmid pPA113-H26R was amplified by PCR with primers nSN27 (GAAATGCTGCAGCCCGTGAGCATGGATATAAGCG ATTTTAT) and nSN28 (GTTAGGTACCAAGCTTGATGGTTCACCTT TTGGC). PCR fragments were digested with KpnI and PstI and inserted into plasmid pAG17 DNA digested with the same two enzymes.

**Chemotaxis assays.** The chemotactic abilities of strains were measured on semisolid tryptone agar plates (20). Where necessary to select for retention of plasmids, plates contained ampicillin (50  $\mu\text{g/ml}$ ) or chloramphenicol (25  $\mu\text{g/ml}$ ).

**Protein purification.** CheA1-149 was purified from cultures of strain RP3098 carrying plasmid pAG3 as described previously (9). Cells were grown in HCG plus 50  $\mu\text{g/ml}$  ampicillin to mid-exponential phase, induced by the addition of IPTG to a final concentration of 200  $\mu\text{M}$ , and grown for an additional 4 h. The cells were harvested by centrifugation, resuspended in buffer A (50 mM Tris-HCl [pH 7.5], 5 mM EDTA, 2 mM  $\beta$ -mercaptoethanol), and passed twice through a French press (10,000 lb/in<sup>2</sup>). The extracts were clarified by centrifugation at 100,000  $\times g$  for 1 h and then precipitated with ammonium sulfate at 45% saturation. The precipitate was resuspended in buffer A, dialyzed against buffer A, and loaded onto a 50-ml column packed with Q-Sepharose (Sigma). After

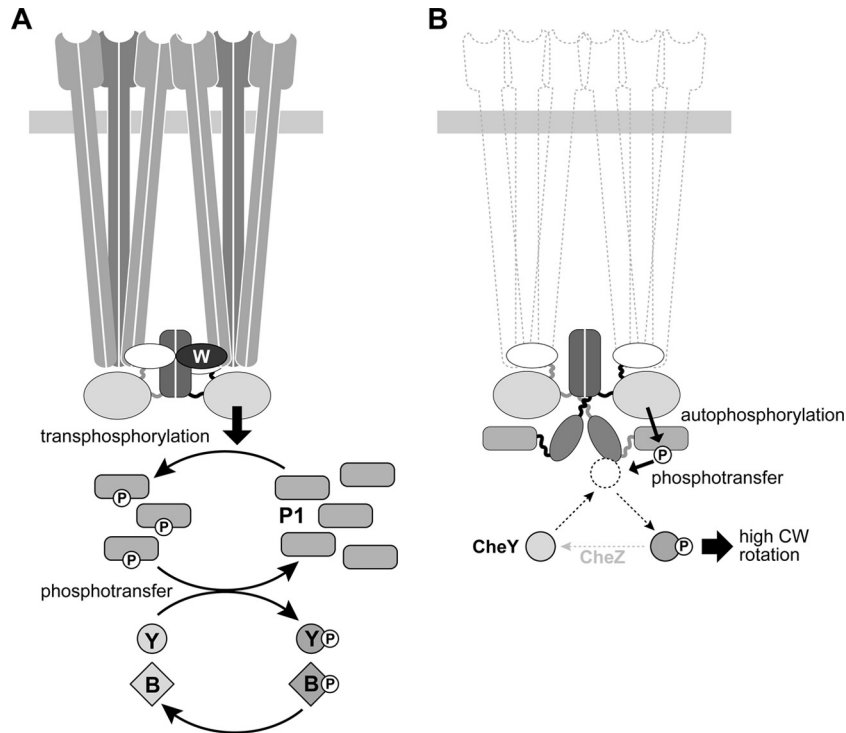


**FIG 2** Phenotypic screens for P1 mutants with phosphorylation defects. (A) Chemotactic signaling by liberated P1 domains. CheA molecules deleted for the P1 and P2 domains couple to chemoreceptors and can phosphorylate free P1 domains in a transphosphorylation reaction. At high expression levels, P1 domains can act as a reservoir of signaling phosphates, passing them to CheY and CheB for behavior control. (B) Pseudotactic control of flagellar rotation by CheA in the absence of chemoreceptors and the CheZ phosphatase. Basal activity of CheA is sufficient, in the absence of CheZ-accelerated dephosphorylation of phospho-CheY, to generate high levels of clockwise flagellar rotation. Reductions in CheA activity lead to lower CW rotation and pseudotactic spreading through soft agar (see the text).

washing with 10 volumes of TEDG10 buffer (50 mM Tris-HCl [pH 7.5], 0.5 mM EDTA, 2 mM dithiothreitol, 10% [vol/vol] glycerol), protein was eluted with a 0 to 400 mM KCl gradient in TEDG10. Fractions containing CheA1-149 were pooled, concentrated, and dialyzed against TEDG10. To avoid proteolytic degradation, 1 mM phenanthroline and 1 mM phenylmethylsulfonyl fluoride were present throughout the purification. Purified CheA260-537 (P3-P4 domains) was a gift from Ron Swanson. CheY protein was purified from cultures of RP3098 carrying plasmid pRL22 as described previously (8).

**Phosphorylation assays.** All reactions were carried out in phosphorylation buffer (50 mM Tris-HCl [pH 7.5], 50 mM KCl, 5 mM MgCl<sub>2</sub>) at room temperature. Assays of transphosphorylation of CheA1-149 by CheA260-537 were performed in 20  $\mu$ l of phosphorylation buffer as described previously (9). Final reactant concentrations were 10  $\mu$ M for P1 fragments and 10  $\mu$ M for P3-P4 fragments. After mixing the purified proteins, reactions were started by addition of  $\gamma$ -<sup>32</sup>P-labeled ATP (~1,000 cpm/pmol) to a final concentration of 1 mM. Phosphotransfer assays between phosphorylated CheA1-149 and CheY were performed as described previously (9). Final reactant concentrations were 1  $\mu$ M for phospho-P1 and 10  $\mu$ M for CheY. At various times, 2- $\mu$ l samples were removed and added to 10  $\mu$ l of sodium dodecyl sulfate (SDS) protein sample buffer (22) to stop the reaction. Reaction products were separated by electrophoresis on sodium dodecyl sulfate-containing 16.5% polyacrylamide gels (SDS-PAGE) and quantified with a Molecular Dynamics PhosphorImager (23).

**Protein modeling and structural display.** *E. coli* CheA homology models were generated from *T. maritima* coordinates by the Swiss-model server (<http://swissmodel.expasy.org>). Structure images were prepared with MacPyMOL software (<http://www.pymol.org>).

## RESULTS

We used two approaches to identify CheA-P1 residues that play functionally important roles in its phosphorylation by the P4 domain or in subsequent phosphotransfer to CheY and CheB.

**Mutant hunt with liberated CheA-P1 domains.** In the first approach, we looked for mutations that disabled the ability of plasmid-encoded P1 fragments (pAG17) to support chemotaxis in a host strain (UU1118) that carries a P3-P4-P5 fragment of CheA (Fig. 2A). This CheA fragment efficiently phosphorylates isolated P1 domains (9) and can support chemotaxis even in the absence of a P2 domain, which is not essential for CheY/CheB phosphorylation or for chemotactic signaling (10, 17). We reasoned that P1 lesions that impaired either the interaction with P4 during autophosphorylation or the subsequent phosphotransfer reactions with CheY and/or CheB should have more drastic signaling consequences in the absence of a covalent connection between P1 and the rest of the CheA molecule. Thus, the liberated P1 system should enable us to detect P1 structural alterations that might have little or no functional effect in the context of the intact protein.

We induced mutations with hydroxylamine in plasmid pAG17 and transformed strain UU1118 with the mutant plasmid pools. At 1 mM IPTG induction, the parental plasmid supports chemotactic signaling in this strain. We screened for pAG17 mutants that could not support chemotaxis in the bipartite CheA setup by plating transformant colonies directly in tryptone semisolid agar con-

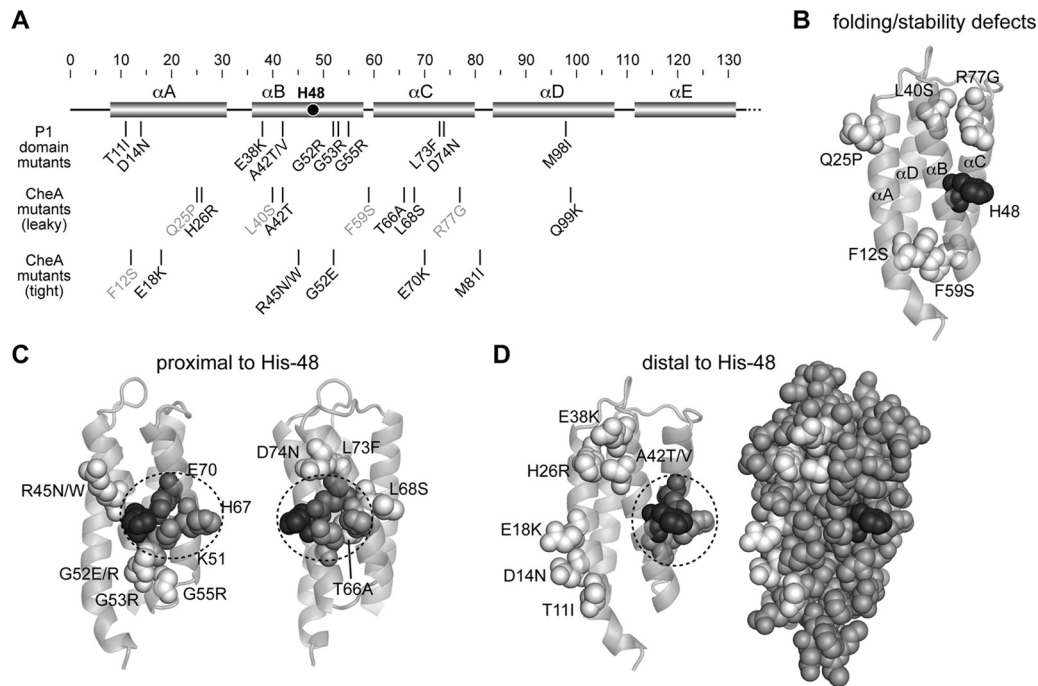


**FIG 3** Summary of P1 lesions obtained from the mutant hunts. (A) Locations of inferred amino acid changes in the primary structure of the P1 domain. Cylindrical segments represent alpha helices; the scale above indicates their P1 residue coordinates. P1 domain mutants were isolated from the P1 plasmid pAG17 using the liberated P1 screen. CheA mutants were isolated from the full-length *cheA* plasmid pPA113 using the pseudotaxis screen. Upon subsequent testing, the pseudotaxis mutants fell into two groups, defined by leaky or tight functional defects. Gray text labels indicate amino acid replacements that reduce steady-state P1 levels in the cell. (B) Arrangement of alpha-helices A to D in the P1 atomic structure (36). His-48 (black atoms) and five presumptive stability lesions (white atoms) are shown in space-fill mode. (C) Locations of P1 alterations (white atoms) that are proximal to His-48 (black) and K51, H67, and E70 (dark gray). The catalytic pocket for autophosphorylation is outlined with a dashed circle. The two structures differ by slight rotation about the vertical axis. (D) Locations of P1 alterations (white atoms) that are distal to His-48 (black) and the catalytic pocket (dashed circle). Both structures are shown in the same orientation. All P1 C, N, and O atoms are space filled on the right to indicate the surface location of the mutant residues.

taining 1 mM IPTG to fully induce P1 expression. Cells that received a mutant P1 plasmid formed small, dense colonies within a diffuse background of chemotaxis-competent cells (not shown). All mutant candidates were then tested for production of P1 protein upon full IPTG induction (see Materials and Methods). Approximately 50% of the initial candidates failed to make detectable levels of P1 product and were not characterized further. The mutational changes in the remaining mutant plasmids were determined by DNA sequencing; all corresponded to single amino acid replacements in P1.

**Hunt for leaky CheA mutants.** In a second mutant hunt, we looked for lesions in the P1 coding region of full-length *cheA* that impaired, but did not eliminate, CheA's ability to generate phospho-CheY. In a host lacking chemoreceptors, the basal autophosphorylation activity of CheA does not produce enough steady-state phospho-CheY to support clockwise (CW) flagellar rotation (24, 25). In contrast, receptorless strains that also lack CheZ, the phospho-CheY phosphatase, have high steady-state levels of phospho-CheY and exhibit nearly incessant CW rotation (4) (Fig. 2B). We reasoned that CheA defects that impaired autophosphorylation or phosphotransfer to CheY should allow more episodes of CCW rotation, thereby enabling the cells to spread in soft agar (25), a behavior termed pseudotaxis (26). Importantly, CheA lesions that completely abolish CheY phosphorylation would cause incessant CCW rotation. Such strains do not spread as rapidly in soft agar as those with balanced CW-CCW behaviors. Thus, the

pseudotaxis screen enabled us to find CheA mutants with leaky phosphorylation or phosphotransfer defects.

We induced random mutations in *cheA* plasmid pPA113 by passage through a *mutD* host and then excised and recloned the P1 coding region to eliminate mutations in other parts of *cheA*. Alternatively, we generated mutations in the P1 portion of the *cheA* coding region of pPA113 by error-prone PCR (27). We transformed strain RP9543 (deleted for *cheA*, all receptor genes, and *cheZ*) with the mutant pools and screened for pseudotactic clones on tryptone soft agar plates (see Materials and Methods). DNA sequencing revealed, in addition to a number of previously isolated alleles, 16 new P1 mutations from this mutant hunt. Most of the pPA113 mutants exhibited partial complementation in RP9535, a *cheA* deletion host, confirming a leaky defect. However, some pPA113 isolates failed to complement RP9535, indicating more complete functional defects (Fig. 3A).

**Identification of possible P4 interaction determinants in the P1 domain.** The inferred amino acid replacements in the P1 mutants obtained from the two mutant hunts fell roughly into three groups based on their P1 expression level and their locations relative to the His-48 phosphorylation site in the P1 tertiary structure (Fig. 3A). Five mutants (F12S, Q25P, L40S, F59S, and R77G) expressed low product levels, most likely due to defects in P1 folding and/or stability (Fig. 3B). We note that F12 and F59 pack against one another in the P1 tertiary structure; L40 and R77 are also close neighbors in the structure (Fig. 3B). These residues lie near helix

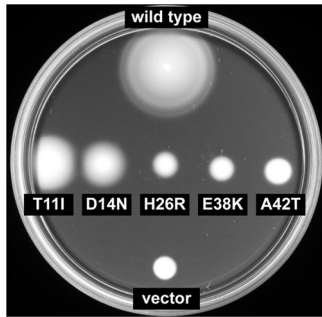


**FIG 4** Chemotactic signaling by liberated mutant P1 domains. Cells of strain UU1118 carrying mutant pAG17 derivatives were tested for chemotactic ability on tryptone medium containing 0.225% agar and 500  $\mu$ M IPTG. The plate was incubated at 30°C for 16 h. The wild-type control plasmid is pAG17; the vector control plasmid is pCJ30.

ends and might serve to stabilize overall P1 structure by promoting packing interactions between the helices. Q25 is more surface exposed on the A helix and probably not important to core packing interactions. However, a proline replacement at this residue would presumably destabilize the helix, which probably accounts for low steady-state levels of the P1-Q25P protein.

Amino acid replacements at nine P1 sites (R45, G52, G53, G55, T66, L68, E70, L73, and D74) involved residues proximal to His-48, the phosphorylation target site, and to residues that play important roles in the catalytic pocket (Fig. 3C). Glu-70 participates in catalyzing the autophosphorylation reaction; Lys-51 and His-67 align reactants in the catalytic pocket (28, 29) (Fig. 3C). Owing to their proximity to these important autophosphorylation determinants, this group of P1 lesions might interfere directly with the CheA phosphorylation and/or phosphotransfer reactions and is not discussed further in this report.

A third set of amino acid replacement sites (T11, D14, H26, E38, A42, M81, M98, and Q99) involved residues more distal to His-48 in the P1 tertiary structure (Fig. 3D). Replacements at Met-81, Met-98, and Gln-99 could affect the orientation of helix D to the other helices of the P1 bundle. Met-81 lies in the loop connecting helices C and D. The side chain of Met-98 (helix D) projects into the core of the 4-helix bundle, and the side chain of Gln-99 (helix D) packs against residues in helix A (not shown). In con-

trast, the side chains of Thr-11, Asp-14, His-26, Glu-38, and Ala-42 were located on the P1 surface along one face of helix A and at the start of helix B (Fig. 3D). These residues could conceivably define a functionally important interaction surface that is distinct from the His-48 phosphorylation pocket (Fig. 3C and D). The signaling phenotypes of these P1 mutants in the liberated domain chemotaxis setup are illustrated in Fig. 4. The H26R replacement, originally isolated in full-length CheA, was also transferred to plasmid pAG17 and was included in these tests. By this functional measure, mutants H26R, E38K, and A42T have more severe defects than do mutants T11I and D14N.

**Biochemical defects of mutant P1 domains.** To test the interaction surface hypothesis, we purified P1 fragments with lesions in  $\alpha$ A (T11I, D14N, H26R) or  $\alpha$ B (E38K, A42T) and examined their phosphorylation properties *in vitro*. When paired with a P4-containing fragment of CheA (CheA260-537), all mutant P1 fragments became phosphorylated, but they did so at lower rates than did a wild-type P1 fragment (Fig. 5A). The phosphorylation rates of the mutant P1 fragments ranged from 6% (E38K) to 36% (T11I) of the wild-type rate. These results indicate that the mutant P1 fragments with amino acid replacements distal to His-48 are less effective substrates for phosphorylation by the ATP-binding and catalytic domain of CheA.

We next examined the abilities of the phosphorylated P1 fragments to donate their phosphoryl groups to CheY by monitoring the kinetics of the transfer reaction through the loss of phosphate label from the P1 donor fragments. In this assay, the mutant P1 fragments showed essentially wild-type or even slightly faster dephosphorylation rates (Fig. 5B). Dephosphorylation of P1 on this time scale was strictly CheY dependent (data not shown), which excludes the possibility that the phosphorylated mutant fragments were unstable in some way. These results indicate that the mutant P1 fragments, once phosphorylated, are not defective as phosphodonor to CheY. We cannot, however, fully discount the possibility that CheY caused dephosphorylation of P1 by some alternative route, for example, by promoting phospho-P1 hydrolysis.

## DISCUSSION

We conducted two independent mutant hunts to identify structural determinants in the CheA P1 domain that might promote its interaction with the ATP-binding P4 domain during the CheA

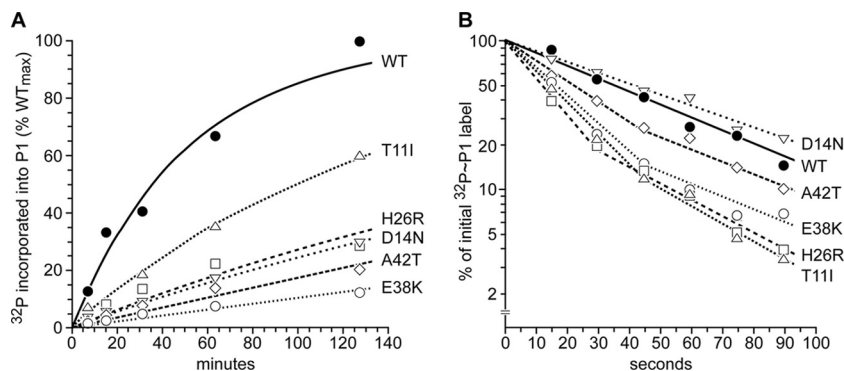


**FIG 5** Transphosphorylation and phosphotransfer activities of mutant P1 domains. Symbols: closed circles, wild type; closed squares, T11I; closed triangles, D14N; open circles, E38K; open squares, A42T. Data points are means from two experiments. See Materials and Methods for experimental details. (A) Transphosphorylation of P1 domains by P3-P4-P5 CheA fragments. Solid lines connecting data points represent nonlinear least-square best fits to the following equation: fraction phosphorylated =  $1 - e^{-k \cdot t}$ , where  $t$  is reaction time in minutes and  $k$  is the pseudo-first-order rate constant for the reaction. (B) Phosphotransfer between phospho-P1 fragments and CheY. Solid lines connecting data points were drawn by hand.

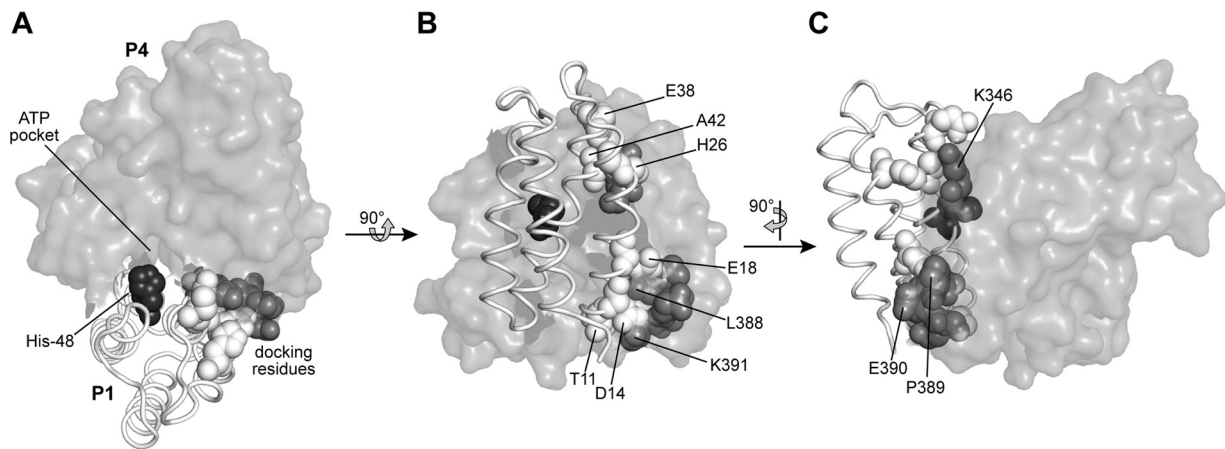


**FIG 6** P1-P4 docking model. Atomic coordinates for the *E. coli* P1-P4 complex were obtained by threading *E. coli* CheA domains onto the modeled *T. maritima* P1-P4 complex of Zhang et al. (7). The P4 domain is shown in surface representation, with key residues for docking P1 shown as dark gray. The P1 domain is shown in backbone trace with key docking residues shown as white. The His-48 phosphorylation site is black. (A) Top view looking down on the 4-helix P1 bundle. (B) Side view showing all putative P1 docking residues identified in this study and two putative P4 docking residues (L388 and K391). (C) A different side view showing other putative P4 docking residues (K346, P389, and E390).

autophosphorylation reaction. One set of signaling-defective P1 mutants had amino acid replacements near the His-48 phosphorylation site. These lesions might alter the positioning of catalytic determinants important for the CheA autophosphorylation and/or phosphotransfer reactions and were not analyzed further in the present study. Another set of P1 mutants had amino acid replacements more distal to His-48, mainly at surface residues in helix A and the start of helix B (Fig. 3D). These mutant P1 domains had reduced rates of transphosphorylation by P3-P4 fragments of CheA (Fig. 5A), but, once phosphorylated, they donated their phosphoryl groups to CheY at unimpaired rates (Fig. 5B). We conclude that these P1 residues define docking determinants that promote interaction with the P4 domain during the CheA autophosphorylation reaction.

**A model of the productive P1-P4 docking interaction.** Zhang et al. developed a model of the productive P1-P4 complex based on docking and molecular dynamics simulations between domains of *Thermotoga maritima* CheA (7, 30). We threaded the *E. coli* P1 and P4 primary structures onto atomic coordinates of their modeled P1-P4 complex and found that our experimental findings were fully consistent with their model (Fig. 6). In particular, the side chain and/or backbone atoms of residues T11, D14, E18, H26, E38, and A42 all abut one or more P4 surface residues in the modeled complex. Three of the five putative P4 interaction sites are charged residues (K346, E390, and K391), and five of their six presumptive P1 partner residues are polar (T11, D14, E18, H26, and E38), suggesting that ionic and hydrogen-bonding interactions play predominant roles in P1-P4 docking.

We constructed several amino acid replacements at P1 residue E38 in plasmid pAG17 (CheA-P1) and at P4 residue K346 in plasmid pSN9 (CheA-P3-P4-P5) to examine their functional interactions in the context of the P1-P4 docking model. The model predicts that some amino acid replacements at either position, for example, ones like alanine that have a small side chain, might not destroy function, given that multiple P1 residues mediate the interaction with P4 (Fig. 6). However, more drastic structural changes, such as charge reversals, might have more deleterious effects on the docking interaction. These are the phenotypic pat-

terns we observed (Fig. 7). For example, an alanine replacement at either position retained function in combination with a wild-type partner, but together the mutant CheA fragments could not complement. The phenotypic specificity of the E38-K346 mutant combinations that we tested is certainly consistent with a structural interaction between these P1 and P4 residues of CheA.

A cysteine-scanning study of *Salmonella enterica* serovar Typhimurium CheA, whose P1 domain is nearly identical to that of *E. coli* CheA, is also consistent with our docking interpretation (6). Miller et al. found that a cysteine replacement at residue A42 of P1, a predicted docking determinant, abrogated CheA signaling (6). In contrast, replacements at D17, Q25, and A37, which are one residue displaced from predicted docking residues E18, H26, and

		P1				
		E38	D	A	R	K
P4	K346	++	++	++	+	+
	R	++	++	++	+	+
	A	++	+	-	-	-
	D	+	-	-	-	-
	E	+	-	-	-	-

**FIG 7** Phenotypic interactions between mutant P1 and P4 domains. Site-directed mutations were created at codon 38 of plasmid pAG17 (P1) and at codon 346 of plasmid pSN9 (P3-P4-P5) to produce the indicated amino acid replacements. Mutant plasmids were tested in all pairwise combinations for the ability to complement the host strain RP9535 ( $\Delta$ cheA). Plasmid-containing cells were tested for chemotaxis on tryptone soft agar plates containing 0.5  $\mu$ M sodium salicylate (to induce P1 expression) and 200  $\mu$ M IPTG (to induce P3-P4-P5 expression). Plates were incubated at 35°C for 9.5 h before scoring with the following system: ++, colony diameter of >75% of that of the wild type with a ring of chemotactic cells at the periphery; +, colony diameter of 40 to 75% of that of the wild type with a chemotactic ring; -, colony diameter of <40% of that of the wild type, no chemotactic ring.

E38 (Fig. 6B), did not impair CheA function, even when modified with a bulky fluorescein (6). In the docking model (7), the side chains of these latter residues should project away from the P1 surface and would probably not be critical to the docking interface with P4 (Fig. 6B). Finally, a cysteine replacement at Q10, adjacent to putative docking residue T11, “hyperactivated” CheA autophosphorylation (6). The Q10C change could conceivably promote productive interactions with the P4 domain by influencing the packing stability of the N terminus of P1 helix A to enhance accessibility of docking determinants. Consistent with this idea, Q10C formed disulfide bonds to several P4 residues, demonstrating collisional interactions between this region of P1 and the P4 domain (31).

The N terminus of P1 helix A has also been implicated in an interaction with CheY (32, 33). In a cocrystal structure of CheA3 and CheY6 of *Rhodobacter sphaeroides*, residue L14 of CheA3, which corresponds to T11 of *E. coli* CheA, makes specific contacts to CheY6 residues (33). Nuclear magnetic resonance (NMR) chemical shift and site-directed spin labeling experiments have also demonstrated that residues T11 and D14 of *E. coli* P1 contact CheY (32). Even if the docking surfaces for P1-P4 and P1-CheY overlap at the beginning of helix A, the two interaction surfaces do not have to be mutually exclusive, because the P4 domain and CheY would not have to bind to P1 at the same time. Thus, the N terminus of P1 helix A might play dual signaling roles. However, we did not detect any phosphotransfer defects for the D14N and T11I mutant P1 domains in the present study, suggesting that interactions between these P1 residues and CheY are not very critical for CheA signaling.

**Evidence for a nonproductive P1-P4 interaction.** Hamel et al. identified residues in *T. maritima* CheA that exhibited NMR chemical shifts upon mixing P1 and P3-P4 fragments (34). They observed chemical shift perturbations of residues in P1 helix A and in the turn between helices A and B, consistent with our mutant results and the Zhang et al. docking model (7) (Fig. 6). However, the largest P1 chemical shifts occurred in helix D residues opposite the phosphorylation site in helix B (34). Moreover, the predominant chemical shifts in P3 and P4 residues defined a P1 interaction site far from the ATP-binding pocket. Hamel et al. suggested that P1 helix D promotes a nonproductive binding interaction with P3-P4 and that receptors modulate this inhibitory interaction to control CheA activity in ternary signaling complexes (34).

**Mechanisms of CheA control in receptor signaling complexes.** Recent cryoelectron microscopy studies of receptor arrays locked in different signaling states revealed that the P1 and P2 domains of CheA are mobile in the kinase-on state and much less mobile in the kinase-off state (35). Conceivably, P1 might engage P3-P4 in the nonproductive binding interaction during CheA deactivation. Alternatively, CheA deactivation in ternary complexes might occur through conformational changes that lock P1 in the productive binding interaction described in the present study, blocking release of P1 from P4, which is probably necessary for subsequent phosphotransfer to CheY and CheB.

It might be possible to distinguish these two control mechanisms by searching for P1 alterations that impair CheA deactivation. If the nonproductive P1 binding interaction plays no role in the autophosphorylation reaction, P1 lesions that disrupt that interaction should respond to receptor-mediated activation but not to deactivation. In contrast, if the productive P1-P4 binding interaction underlies both CheA control mechanisms in ternary com-

plexes, alteration of the P1 determinants for that interaction most likely would impair both control responses.

## ACKNOWLEDGMENTS

We thank Jian Zhang (Jiao Tong University School of Medicine) for providing the atomic coordinates for the *T. maritima* P1-P4 docking model.

This work was supported by research grant GM19559 from the National Institute of General Medical Sciences. The Protein-DNA Core Facility at the University of Utah receives support from National Cancer Institute grant CA42014 to the Huntsman Cancer Institute.

## REFERENCES

- Hazelbauer GL, Falke JJ, Parkinson JS. 2008. Bacterial chemoreceptors: high-performance signaling in networked arrays. *Trends Biochem. Sci.* 33:9–19. <http://dx.doi.org/10.1016/j.tibs.2007.09.014>.
- Wadhams GH, Armitage JP. 2004. Making sense of it all: bacterial chemotaxis. *Nat. Rev. Mol. Cell Biol.* 5:1024–1037. <http://dx.doi.org/10.1038/nrm1524>.
- Swanson RV, Bourret RB, Simon MI. 1993. Intermolecular complementation of the kinase activity of CheA. *Mol. Microbiol.* 8:435–441. <http://dx.doi.org/10.1111/j.1365-2958.1993.tb01588.x>.
- Zhao J, Parkinson JS. 2006. Mutational analysis of the chemoreceptor-coupling domain of the *Escherichia coli* chemotaxis signaling kinase CheA. *J. Bacteriol.* 188:3299–3307. <http://dx.doi.org/10.1128/JB.188.9.3299-3307.2006>.
- Zhao J, Parkinson JS. 2006. Cysteine-scanning analysis of the chemoreceptor-coupling domain of the *Escherichia coli* chemotaxis signaling kinase CheA. *J. Bacteriol.* 188:4321–4330. <http://dx.doi.org/10.1128/JB.00274-06>.
- Miller AS, Kohout SC, Gilman KA, Falke JJ. 2006. CheA Kinase of bacterial chemotaxis: chemical mapping of four essential docking sites. *Biochemistry* 45:8699–8711. <http://dx.doi.org/10.1021/bi060580y>.
- Zhang J, Xu Y, Shen J, Luo X, Chen J, Chen K, Zhu W, Jiang H. 2005. Dynamic mechanism for the autophosphorylation of CheA histidine kinase: molecular dynamics simulations. *J. Am. Chem. Soc.* 127:11709–11719. <http://dx.doi.org/10.1021/ja051199o>.
- Morrison TB, Parkinson JS. 1994. Liberation of an interaction domain from the phosphotransfer region of CheA, a signaling kinase of *Escherichia coli*. *Proc. Natl. Acad. Sci. U. S. A.* 91:5485–5489. <http://dx.doi.org/10.1073/pnas.91.12.5485>.
- Garzon A, Parkinson JS. 1996. Chemotactic signaling by the P1 phosphorylation domain liberated from the CheA histidine kinase of *Escherichia coli*. *J. Bacteriol.* 178:6752–6758.
- Stewart RC, Jahreis K, Parkinson JS. 2000. Rapid phosphotransfer to CheY from a CheA protein lacking the CheY-binding domain. *Biochemistry* 39:13157–13165. <http://dx.doi.org/10.1021/bi001100k>.
- Cox EC, Horner DL. 1986. DNA sequence and coding properties of *mutD(dnaQ)* a dominant *Escherichia coli* mutator gene. *J. Mol. Biol.* 190:113–117. [http://dx.doi.org/10.1016/0022-2836\(86\)90080-X](http://dx.doi.org/10.1016/0022-2836(86)90080-X).
- Parkinson JS, Houts SE. 1982. Isolation and behavior of *Escherichia coli* deletion mutants lacking chemotaxis functions. *J. Bacteriol.* 151:106–113.
- Smith RA, Parkinson JS. 1980. Overlapping genes at the cheA locus of *Escherichia coli*. *Proc. Natl. Acad. Sci. U. S. A.* 77:5370–5374. <http://dx.doi.org/10.1073/pnas.77.9.5370>.
- Sanatinia H, Kofoid EC, Morrison TB, Parkinson JS. 1995. The smaller of two overlapping cheA gene products is not essential for chemotaxis in *Escherichia coli*. *J. Bacteriol.* 177:2713–2720.
- Morrison TB, Parkinson JS. 1997. A fragment liberated from the *Escherichia coli* CheA kinase that blocks stimulatory, but not inhibitory, chemoreceptor signaling. *J. Bacteriol.* 179:5543–5550.
- Gosink KK, Buron-Barral M, Parkinson JS. 2006. Signaling interactions between the aerotaxis transducer Aer and heterologous chemoreceptors in *Escherichia coli*. *J. Bacteriol.* 188:3487–3493. <http://dx.doi.org/10.1128/JB.188.10.3487-3493.2006>.
- Jahreis K, Morrison TB, Garzon A, Parkinson JS. 2004. Chemotactic signaling by an *Escherichia coli* CheA mutant that lacks the binding domain for phosphoacceptor partners. *J. Bacteriol.* 186:2664–2672. <http://dx.doi.org/10.1128/JB.186.9.2664-2672.2004>.
- Bibikov SI, Biran R, Rudd KE, Parkinson JS. 1997. A signal transducer for aerotaxis in *Escherichia coli*. *J. Bacteriol.* 179:4075–4079.
- Matsumura P, Rydel JJ, Linzmeier R, Vacante D. 1984. Overexpression

- and sequence of the *Escherichia coli cheY* gene and biochemical activities of the CheY protein. *J. Bacteriol.* **160**:36–41.
20. Parkinson JS. 1976. *cheA*, *cheB*, and *cheC* genes of *Escherichia coli* and their role in chemotaxis. *J. Bacteriol.* **126**:758–770.
  21. Wolff C, Parkinson JS. 1988. Aspartate taxis mutants of the *Escherichia coli tar* chemoreceptor. *J. Bacteriol.* **170**:4509–4515.
  22. Laemmli UK. 1970. Cleavage of structural proteins during the assembly of the head of bacteriophage T4. *Nature* **227**:680–685. <http://dx.doi.org/10.1038/227680a0>.
  23. Morrison TB, Parkinson S. 1994. Quantifying radiolabeled macromolecules and small molecules on a single gel. *Biotechniques* **17**:922–926.
  24. Liu JD, Parkinson JS. 1989. Role of CheW protein in coupling membrane receptors to the intracellular signaling system of bacterial chemotaxis. *Proc. Natl. Acad. Sci. U. S. A.* **86**:8703–8707. <http://dx.doi.org/10.1073/pnas.86.22.8703>.
  25. Wolfe AJ, Berg HC. 1989. Migration of bacteria in semisolid agar. *Proc. Natl. Acad. Sci. U. S. A.* **86**:6973–6977. <http://dx.doi.org/10.1073/pnas.86.18.6973>.
  26. Ames P, Yu YA, Parkinson JS. 1996. Methylation segments are not required for chemotactic signalling by cytoplasmic fragments of Tsr, the methyl-accepting serine chemoreceptor of *Escherichia coli*. *Mol. Microbiol.* **19**:737–746. <http://dx.doi.org/10.1046/j.1365-2958.1996.408930.x>.
  27. Cadwell RC, Joyce GF. 1994. Mutagenic PCR. *PCR Methods Appl.* **3**:S136–S140. <http://dx.doi.org/10.1101/gr.3.6.S136>.
  28. Quezada CM, Gradinaru C, Simon MI, Bilwes AM, Crane BR. 2004. Helical shifts generate two distinct conformers in the atomic resolution structure of the CheA phosphotransferase domain from *Thermotoga maritima*. *J. Mol. Biol.* **341**:1283–1294. <http://dx.doi.org/10.1016/j.jmb.2004.06.061>.
  29. Quezada CM, Hamel DJ, Gradinaru C, Bilwes AM, Dahlquist FW, Crane BR, Simon MI. 2005. Structural and chemical requirements for histidine phosphorylation by the chemotaxis kinase CheA. *J. Biol. Chem.* **280**:30581–30585. <http://dx.doi.org/10.1074/jbc.M505316200>.
  30. Shi T, Lu Y, Liu X, Chen Y, Jiang H, Zhang J. 2011. Mechanism for the autophosphorylation of CheA histidine kinase: QM/MM calculations. *J. Phys. Chem. B* **115**:11895–11901. <http://dx.doi.org/10.1021/jp203968d>.
  31. Gloor SL, Falke JJ. 2009. Thermal domain motions of CheA kinase in solution: disulfide trapping reveals the motional constraints leading to trans-autophosphorylation. *Biochemistry* **48**:3631–3644. <http://dx.doi.org/10.1021/bi900033r>.
  32. Mo G, Zhou H, Kawamura T, Dahlquist FW. 2012. Solution structure of a complex of the histidine autokinase CheA with its substrate CheY. *Biochemistry* **51**:3786–3798. <http://dx.doi.org/10.1021/bi300147m>.
  33. Bell CH, Porter SL, Strawson A, Stuart DI, Armitage JP. 2010. Using structural information to change the phosphotransfer specificity of a two-component chemotaxis signalling complex. *PLoS Biol.* **8**:e1000306. <http://dx.doi.org/10.1371/journal.pbio.1000306>.
  34. Hamel DJ, Zhou H, Starich MR, Byrd RA, Dahlquist FW. 2006. Chemical-shift-perturbation mapping of the phosphotransfer and catalytic domain interaction in the histidine autokinase CheA from *Thermotoga maritima*. *Biochemistry* **45**:9509–9517. <http://dx.doi.org/10.1021/bi060798k>.
  35. Briegel A, Ames P, Gumbart JC, Oikonomou CM, Parkinson JS, Jensen GJ. 2013. The mobility of two kinase domains in the *Escherichia coli* chemoreceptor array varies with signalling state. *Mol. Microbiol.* **89**:831–841. <http://dx.doi.org/10.1111/mmi.12309>.
  36. Mourey L, Da Re S, Pedelacq JD, Tolstykh T, Faurie C, Guillet V, Stock JB, Samama JP. 2001. Crystal structure of the CheA histidine phosphotransfer domain that mediates response regulator phosphorylation in bacterial chemotaxis. *J. Biol. Chem.* **276**:31074–31082. <http://dx.doi.org/10.1074/jbc.M101943200>.